

# Proposal to Perform a High-Statistics Neutrino Scattering Experiment Using a Fine-grained Detector in the NuMI Beam

*Version 0.0*

*November 24, 2003*

(list of institutions)

## **Abstract**

The NuMI Facility at Fermilab will provide an extremely intense beam of neutrinos for the MINOS neutrino oscillation experiment. The spacious and fully-outfitted MINOS near detector hall will be an ideal place for a high statistics  $\nu$  and  $\bar{\nu}$ -nucleon/nucleus scattering experiment. The experiment described here will provide the neutrino cross-sections and measured nuclear effects required by on-and-off axis neutrino oscillation experiments. In addition, with the high NuMI beam intensity, the experiment will either initially address or significantly improve our knowledge of a wide variety of neutrino physics topics of interest and importance to both the Elementary Particle and Nuclear Physics communities.



# Contents

List of Figures	v
List of Tables	vii
<b>1 Resonance-Mediated Processes</b>	<b>1</b>
1.1 Overview . . . . .	1
1.2 Expected Results . . . . .	7



## List of Figures

1	Inclusive electron scattering showing $\Delta$ and higher resonances. $Q^2$ at the $\Delta$ peak is approximately 0.5, 1.5, 2.5 and 3.5 (GeV/c) <sup>2</sup> for the four spectra respectively . . . . .	11
2	Invariant mass spectra from $p(e, e'X)$ demonstrating the multi-hadron reconstruction capability in the JLab CLAS spectrometer.[?] . . . . .	12
3	Total pion production cross sections. . . . .	12
4	Predicted $\pi^+$ energy distribution for $\nu_\mu$ scattering on $^{16}\text{O}$ of Paschos et. al.[?]. . . . .	13
5	$W$ and $Q^2$ reconstruction for events with a single $\pi^+$ . Top row are “true” $W$ and $Q^2$ distributions from the MINER $\nu$ A Monte Carlo. The second row are the reconstructed distributions assuming hadron energy resolutions from Figure ?? . The invariant mass of the pion and highest energy proton give $W$ which along with the muon energy and direction gives sufficient information to reconstruct $Q^2$ . Bottom row shows the correlation between the “true” and reconstructed quantities. . . . .	14
6	Single charged pion resolution derived from MINER $\nu$ A Monte Carlo. . . . .	15
7	Differential cross section $d\sigma/dQ^2$ ( $10^{-38}\text{cm}^2/\text{GeV}^2$ ) of $p(\nu_\mu, \mu^-\pi^+)p$ averaged over neutrino energies. Calculations from Ref. [?], data from Ref. [?]. . . . .	16



## List of Tables





# 1 Resonance-Mediated Processes

Inclusive Electron scattering at  $W < 2$  shows (Fig. 1) peaks corresponding to the  $\Delta(1232)$  and higher resonances at low  $Q^2$ . This resonance structure is expected in neutrino scattering, although there is little data to data in this region. As well as the natural interest in studying neutrino induced resonance production, a better understanding is valuable for interpreting modern neutrino experiments. This is particularly the case for neutrinos in the region of 1 GeV, where single pion production comprises about 30% of the total neutrino CC cross section.

Neutrino monte carlo programs in this kinematic region have been using early theoretical predictions by Rein and Seghal. [?] Recently Sato, Uno and Lee[?] have extended a model of electron scattering to the Delta Resonance to weak production. Also, Paschos and collaborators, using the formalism of Schreiner and von Hippel[?] have included the effects of pion rescattering and absorbtion for resonance production in nuclei.

## 1.1 Overview

In electron scattering, the behavior of the  $\Delta(1232)$  resonance transition form factor is considered to be a primary indicator for the onset of perturbative QCD. This is because there is a dramatic discrepancy between the  $Q^2$  behavior expected from a description of this resonance in terms of a spin-flip transition, and the helicity conservation requisite to perturbative descriptions. The various measured elastic and resonance form factors have been compared, and it has been observed [?, ?, ?, ?, ?, 1] that, while the proton and higher mass resonance form factors appear to approach the predicted leading order pQCD  $Q^{-4}$  behavior by around  $Q^2 = 2 \text{ GeV}^2$ , the  $\Delta(1232)$  transition form factor decreases more rapidly with  $Q^2$ . A suggested explanation [?] is that helicity-nonconserving processes are dominating. The  $\Delta$  is primarily a spin-flip transition at low momentum transfer, wherein the helicity-nonconserving  $A_{\frac{3}{2}}$  amplitude is dominant [?]. If the leading order  $A_{\frac{1}{2}}$  helicity-conserving amplitude were also suppressed at large momentum transfers, the quantity  $Q^4 F$  would be expected to decrease as a function of  $Q^2$ .

Helicity is the projection of a particle's spin along its direction of motion. Electromagnetic transition helicity matrix elements correspond to transitions in which the initial state has helicity  $\lambda$  and the final states have helicity  $\lambda'$ .

Transitions between a nucleon state  $|N\rangle$  and a resonant state  $|R\rangle$  can be expressed in terms of dimensionless helicity matrix elements[?]:

$$G_\lambda = \frac{1}{2M} \langle R, \lambda' | \epsilon^\mu J_\mu | N, \lambda \rangle. \quad (1)$$

In this equation, the polarization vectors  $\epsilon^{+, -, 0}$  correspond to right and left circularly polarized photons, and longitudinally polarized photons, respectively. Following the formalism used by Stoler [?] and others, the differential cross section may be written in terms of longitudinal and transverse form factors  $G_E$  and  $G_T$ , as follows:

$$\frac{d^2\sigma}{d\Omega dE'} = \sigma_m f_{rec} \left[ \frac{|G_E|^2 + \tau^* |G_T|^2}{1 + \tau^*} + 2\tau^* |G_T|^2 \tan^2 \left( \frac{\theta}{2} \right) \right] R(W). \quad (2)$$

This is in analogy with the Sachs form factors for elastic scattering. In terms of the dimensionless helicity elements above,

$$G_E = G_0 \quad (3)$$

and

$$\tau^* |G_T|^2 = \frac{1}{2} (|G_+|^2 + |G_-|^2), \quad (4)$$

where

$$\tau^* = \frac{\nu^2}{Q^2}. \quad (5)$$

The recoil factor  $f_{rec}$  is given by

$$f_{rec} = \frac{E'}{E_o}. \quad (6)$$

$R(W)$  is the familiar Breit Wigner formula [?] for the shape of the cross section as a function of energy:

$$R(W) = \frac{2\pi^{-1} W_R M \Gamma_R}{(W^2 - W_R^2)^2 + W_R^2 \Gamma_R^2}. \quad (7)$$

The mass and width of the resonance are  $W_R$  and  $\Gamma_R$ .

Helicity is conserved in vector interactions with free relativistic fermion spinors. In the limit that a spin- $\frac{1}{2}$  parton is massless and free its helicity

must be conserved in interactions with a vector gluon or photon. At sufficient momentum transfer, the constituent quarks within a hadron can be treated as massless and free and the hadron helicity can be treated as the sum of its constituent quark helicities [?, ?]. Therefore, at high  $Q^2$ , hadron helicity is also expected to be conserved.

For resonance electroproduction, the situation can be considered in the Breit frame for the  $\lambda = 3/2$   $\Delta$  resonance. The incoming virtual photon can have positive, zero, or negative helicity. The outgoing resonance helicity can be calculated from angular momentum conservation [?]:

$$\lambda_\Delta = \lambda_\gamma - \lambda_N. \quad (8)$$

Hadron helicity is conserved when the incoming photon helicity is positive, and the  $\Delta$  excitation emerges with the same helicity (1/2) as the initial nucleon state. This is described by the helicity amplitude  $A_{\frac{1}{2}}$  given by:

$$A_{\frac{1}{2}} = \sqrt{\frac{2\pi\alpha}{\kappa}} G_+. \quad (9)$$

$\kappa$  is the energy of an equivalent on-mass-shell (real) photon producing a final mass state W:

$$\kappa = (W^2 - M^2)/2M. \quad (10)$$

Helicity is not conserved when  $A_{\frac{3}{2}}$  given by

$$A_{\frac{3}{2}} = \sqrt{\frac{2\pi\alpha}{\kappa}} G_- \quad (11)$$

is the dominant amplitude.

In terms of helicity amplitudes a dimensionless form factor F may be defined where:

$$F^2 = |G_T(Q^2)|^2 = \frac{1}{4\pi\alpha} \frac{2M}{Q^2} (W_R^2 - M_N^2) |A_H(Q^2)|^2. \quad (12)$$

Here,

$$|A_H(Q^2)|^2 = |A_{\frac{1}{2}}(Q^2)|^2 + |A_{\frac{3}{2}}(Q^2)|^2. \quad (13)$$

At high  $Q^2$ , the helicity conserving amplitude is predicted to dominate the helicity-nonconserving amplitude.  $A_{\frac{3}{2}}$  is predicted to be small compared to  $A_{\frac{1}{2}}$  by pQCD.

In leading order pQCD, two gluons are exchanged among the three point-like quarks. The gluon exchanges ensure that the final quarks, like the initial ones, have low relative momenta, so that no powers of  $Q^2$  come from the wave functions. Form factors calculated in the light-cone frame take the form [?]:

$$F(Q^2) = \int_0^1 \int_0^1 dx dy \Phi(x)^* T_H \Phi(y) \quad (14)$$

where  $x$  and  $y$  are the initial and final longitudinal momentum fractions.  $\Phi(x)$  and  $\Phi(y)$  are the corresponding quark distribution amplitudes and  $T_H$  is the transition operator which is evaluated over all possible leading order diagrams. This leads to the dimensional scaling rule [?]

$$G_+ \propto A_{\frac{1}{2}} \propto Q^{-3}, \quad (15)$$

or

$$F \propto Q^{-4}. \quad (16)$$

This  $Q^2$  dependence of the helicity amplitudes may be established up to factors involving  $\ln(Q^2)$  [?]. At high  $Q^2$  where the quark helicities are conserved,

$$G_+ \propto Q^{-3}, \quad (17)$$

$$G_0 \propto \left(\frac{m}{Q}\right) G_+, \quad (18)$$

and

$$G_- \propto \left(\frac{m^2}{Q^2}\right) G_+. \quad (19)$$

The prediction that  $F(Q^2) \propto 1/Q^4$  if  $G_+$  is dominant can be seen from combining the above with the previous definitions of  $A_{\frac{3}{2}}$  and  $A_{\frac{1}{2}}$  in the dimensionless form factor definition.

In addition to the  $Q^2$  dependence of the transition form factors discussed above, pQCD makes definite predictions about the relative contributions of the magnetic dipole  $M_{1+}$ , electric quadrupole  $E_{1+}$ , and Coulomb quadrupole  $S_{1+}$ , multipole amplitudes. In quark models at low  $Q^2$ , the  $N-\Delta$  transition is due primarily to a single quark spin flip requiring the  $M_{1+}$  to be the dominant contribution [2]. At very low  $Q^2$ , near zero, experiments have confirmed this prediction, evaluating  $E_{1+}$  and  $M_{1+}$  at the resonance position. However, as previously discussed, only helicity conserving amplitudes should contribute at high  $Q^2$ , which leads to the prediction that the ratio  $E_{1+}/M_{1+} = 1$ . Results

from Jefferson Lab [1] indicate that hadron helicity is not yet conserved at  $Q^2 = 4 \text{ GeV}^2$ , finding the transition form factor  $F$  to be decreasing faster than  $Q^{-4}$  and continued  $M_{1+}$  dominance. However, while pQCD apparently does not yet describe resonance excitation at these momentum transfers, it is not clear how constituent quark models can be appropriate at such high  $Q^2$  values, and regardless no single model describes all of the data well. The Delta resonance, then, remains an object of intense study at facilities like Jefferson Lab and Mainz, with future experiments planned.

Sato and Lee [?] have developed a dynamical model for pion photo and electroproduction in the region of the  $\Delta$  resonance which is used to extract  $N - \Delta$  transition form factors. Through this work, the afore-mentioned discrepancy between the  $\Delta$  transition form factor as calculated from a constituent quark model and the measured transition form factor (a difference of about 35%) has been understood by including a dynamical pion cloud effect. Recently this work has been extended by Sato, Uno and Lee to weak pion production [?]. They show that the renormalized axial  $N - \Delta$  form factor contains large dynamical pion cloud effects which are crucial in obtaining agreement with the available data (in this case, on hydrogen and deuterium). Contrary to previous observations, they conclude that the  $N - \Delta$  transitions predicted by the constituent quark model are consistent with existing neutrino-induced pion production data in the  $\Delta$  region. It is interesting to note that the pion cloud effect on the axial  $N - \Delta$  form factor is mainly to increase the magnitude. On the other hand, both the magnitude and the slope of the  $M_{1+}$  are significantly changed by including pion cloud effects. The authors site the need for more extensive and precise data on neutrino-induced pion production reactions in order to test their model and to pin down the  $Q^2$ -dependence of the axial vector  $N - \Delta$  transition form factor - data which MINER $\nu$ A will certainly provide.

The MINER $\nu$ A data will be on nuclei, at least in the first years without a hydrogen target, and comparison to improved data on a free proton target will not be possible. Nonetheless, as discussed in the duality section, the average  $Q^2$  dependence of the cross sections (and, hence, structure functions and transition form factors) will be made more manifest by the Fermi smearing of the resonance enhancements. Therefore, it should be possible to pin down the  $Q^2$ -dependence of the axial vector  $N - \Delta$  transition form factor. Moreover, the work of Sato, Uno and Lee, can be used as Monte Carlo input for MINER $\nu$ A, and should be a crucial ingredient to predictions of delta excitation in nuclei which can be compared directly with MINER $\nu$ A data.

Neutrino experiments rely heavily on detailed Monte Carlos to simulate the response of the rather complicated target / detector systems involved. The MINER $\nu$ A simulation will be greatly enhanced by accurate descriptions of the nuclear effects involved. The majority of hadrons produced in inelastic scattering are pions, and so the nuclear attenuation of these must be taken into account. In considering hadron attenuation results from HERMES, Gaskell [?] suggests that a good first step is the one time scale parameterization, which goes as  $(1 - z)\nu$ . The A-dependence could then be taken into account via a simple  $A^{2/3}$  scaling in  $(1 - R_A)$ , where  $R_A$  is the ratio of cross section on nucleus A to deuterium.

Another relevant nuclear effect, currently being applied in neutrino event generators [] for protons but not pions, is termed color transparency (CT). Color transparency, first conjectured by Mueller and Brodsky [3] refers to the suppression of final (and initial) state interactions of hadrons with the nuclear medium in exclusive processes at high momentum transfers. CT is an effect of QCD, related to the presence of non-abelian color degrees of freedom underlying strongly interacting matter. The basic idea is that, under the right conditions, three quarks (in the case of the proton), each of which would normally interact strongly with the nuclear medium, can form an object that passes undisturbed through the nuclear medium. This small object would be color neutral outside of a small radius in order not to radiate gluons. Unambiguous observation of CT would provide a new means to study the strong interaction in nuclei.

Several measurements of the transparency of the nuclear medium to high energy protons have been carried out in the last decade. At Jefferson Lab, CT searches have concentrated on the quasi-elastic  $A(e, e'p)$  reaction which has several advantages in the search for CT. To date,  $A(e, e'p)$  experiments at SLAC [4] and JLab [5] have found no evidence for the onset of CT at momentum transfers up to 8.1 GeV<sup>2</sup>. However, there is some potential evidence for CT in  $A(p, 2p)$  data from Brookhaven [6, 7].

It has been suggested that the onset of CT will be sooner in a  $q\bar{q}$  system than in a three-quark system. Thus, the next best reaction in the expectation of CT is the  $A(e, e'\pi)$  reaction. Current theoretical calculations suggest that most of this CT effect should be seen around  $Q^2 = 10$  (GeV/c)<sup>2</sup>, well within the MINER $\nu$ A kinematic range. This effect has not yet been considered in neutrino Monte Carlos, nor has it been well studied in other processes. However, it will be well-measured in the Jefferson Lab kinematic regime prior to MINER $\nu$ A [8], and should then be incorporable into the Monte Carlo.

While there is a large body of inclusive  $(e, e')$  scattering data in the resonance region on hydrogen, deuterium and nuclei, more exclusive measurements have been rare until recently. With JLab  $p(e, e'p)\pi^0$  spectrometer measurements[?, 1], the CLAS  $N^*$  program[?] and CLAS  $^{12}\text{C}(e, e'X)$  data, more exclusive reactions are becoming available. This data will help to “calibrate” the Vector current part of weak resonance/meson production models and to extend Delta resonance models such as that of Sato, Uno and Lee to higher resonances. These exclusive measurements are also naturally of interest because even to make inclusive measurements with neutrinos, the full final state must be observed and reconstructed. With the expected statistics and resolution of MINER $\nu$ A, it should thus be possible to extract much more information about resonances than what is available in the inclusive channel.

Figure 2 from the CLAS[?] is an illustration of the type of just part of the information available when one or more reaction fragments are detected in resonance region electron scattering. One item of interest in this data is a peak observed near  $W = 1.72\text{GeV}$  in the spectrum for the  $p\pi + \pi^-$  final state. While an analysis of the angular distribution of this peak gives quantum numbers that agree with the PDG  $N_{3/2+}^*(1720)$  state, the observed hadronic properties (coupling amplitudes) of this resonance are quite different from what is predicted from the PDG state. This illustrates that electro-weak excitation of baryon resonances is an active field and that MINER $\nu$ A measurements are timely.

## 1.2 Expected Results

Resonance production measurements in MINER $\nu$ A can be grouped into two categories:

1. Measurement of inclusive  $(\nu_\mu, \mu^-)$  and  $(\nu, \nu)$  spectra in the resonance region. As is done in the deep-inelastic region, this implies extraction of structure functions which can be compared to structure functions and form factors from electron scattering. The experimental method same is the same as for DIS events. For each event, we sum up the energies and momenta of the muon and all final state hadrons to get the total neutrino energy, and calculate  $Q^2$  and  $W$ ,  $y$  etc. This kind of analysis will be done as a function of  $W$  for the entire resonance region.
2. Examination of specific final state reaction products (single pion production, inclusive pion spectra). Specific final states are useful in selec-

tion of a specific final state isospin. This kind of analysis is primarily aimed at single pion production in the region of the first resonance.

The analysis of each of the above two types of measurements categories will be closely coordinated with complementary experiments at Jefferson Laboratory (which are led by members of the MINER $\nu$ A collaboration). The following are the Jefferson Laboratory electron scattering experiments in Hall C that are connected with measurements of inclusive scattering in the resonance region at MINER $\nu$ A.

1. JLab hydrogen experiment E94-110 (investigates inclusive  $F_2$  and  $R$  in the resonance region). C.E. Keppel spokesperson (data already taken).
2. JLab deuterium experiment E02-109, investigates inclusive  $F_2$  and  $R$  in the resonance region. C.E. Keppel, M. E. Christy, spokespersons (approved to run in 2004).
3. JLab experiment E99-118 investigates nuclear the dependence of  $F_2$  and  $R$  at low  $Q^2$  for high values of  $W$ . A. Brull, C.E. Keppel spokespersons (data already taken).
4. Jlab experiment E02-103 hydrogen and deuterium resonance  $F_2$  data at high  $Q^2$  approved by Jlab PAC24 to run in 2004 (J. Arrington, spokesperson)
5. Jlab Proposal PR03-110 to investigate  $F_2$  and  $R$  in the resonance region with nuclear targets. A. Bodek and C. E. Keppel, spokespersons (proposed to run in Hall C together with E02-109 in 2004) to provide vector resonance form factors and  $R$  on the same nuclear targets that are used in neutrino experiments (e.g. Carbon, Iron, Lead).

The following are collaborative programs between the electron scattering community that are connected with measurements of final states in the quasielastic region and in the region of the first resonance at MINER $\nu$ A.

1. Steve Manly (Rochester) and Will Brooks (Jlab) program to use existing Hall B CLAS data at Jefferson Laboratory to study hadronic final states in electron scattering on nuclear targets (e.g. Carbon).



2. Work with the Argonne group of Lee to model first resonance production in the region of the first resonance and also Ghent nuclear physics group in Belgium [?], to model both electron and neutrino induced final states. In addition, there are other theoretical efforts (e.g. Sakuda and Paschos) on nuclear effects for the hadronic final states in the region of the first resonance.
3. Comparison of electron scattering data (primarily proton and pion transparency measurements) to final state interaction models used in neutrino event generators such as NUANCE and NEUGEN.[?]

The analysis of inclusive data in the resonance region with MINER $\nu$ A will be done using the standard structure function analysis techniques. The sum of neutrino and antineutrino differential cross sections is used to do a Rosenbluth separation and extract  $F_2$  and  $R$  for a Carbon target. The difference between neutrino and antineutrino differential cross sections is used to extract the structure function  $xF_3$ . The nuclear effects in the resonance region at low values of  $Q^2$  are not well understood. Electron scattering data show that duality works at  $Q^2$  greater than 1 (GeV/c) $^2$  for hydrogen and deuterium targets. In addition, there are indications that the nuclear effects also scale with the Nachtmann scaling variable. However, these observations have not been tested in neutrino scattering, nor have they been tested in neutrino or electron scattering at lower values of  $Q^2$ . The information from Jefferson Laboratory proposal E03-110 will provide this information for nuclear targets for the vector structure functions. MINER $\nu$ A in turn will be able to extend these duality studies to the axial vector structure functions.

At present, the axial form factor for the first resonance is not very well known. MINER $\nu$ A will have a very high statistics sample in this region, which is equivalent to the sample for quasilelastic scattering described earlier. However, since MINER $\nu$ A data is on a Carbon target, nuclear effects must be understood. The theoretical tools used to model the nuclear effects in Carbon for the final state particles in the region of the first resonance in neutrino scattering, will be tested with CLAS Hall B electron scattering Jefferson Lab data on Carbon and other electron scattering data.

Using the angular distribution in the exclusive final states  $\nu_\mu p \rightarrow \mu^- \pi^+ p$ , we plan to fit for the resonant and non-resonant amplitudes. The extracted non-resonant amplitude should be consistent with the measured value of  $R$  in this region (extracted from the inclusive scattering sample).

By using both neutrino and antineutrino data MINER $\nu$ A can investigate transitions into isospin 3/2 states  $\Delta^{++}$  and  $\Delta^{-}$ . An analysis of the ratios of various final states.  $p\pi^{+}$ ,  $n\pi^{+}$  and  $p\pi_0$  will provide additional information. As mentioned earlier, we plan to do a comparison of resonance production with electron scattering on free nucleons to Hall B CLAS data with bound nucleons in Carbon. Within MINER $\nu$ A itself, we can compare the reactions  $\nu p \rightarrow \nu n\pi^{+}$  and  $\nu n \rightarrow \nu p\pi^{-}$  on bound nucleons directly, and investigate additional channels in order to better understand the effects of pion and nucleon rescattering.

MINER $\nu$ A is expected to have good resolution for single pion events in the resonance region ( $W \lesssim 2$  GeV/c). Figure 5 shows  $Q^2$  and  $W$  distributions of single pion events from CH<sub>2</sub> in the MINER $\nu$ A Monte Carlo along with reconstructed distributions that take into account MINER $\nu$ A's energy resolution for hadrons. (Fig. 6) While the Fermi motion in nuclei washes out higher resonances, it is clear that Delta events can be readily identified and separated from higher resonances. This expected resolution implies that a differential cross section  $d\sigma/dQ^2$  for Delta production on Carbon equivalent to that for Hydrogen (Fig. 7) can be obtained with high statistics.

## References

- [1] V. V. Frolov *et al.*, Phys. Rev. Lett. **82**, 45 (1999)
- [2] C. Becchi and G. Morpurgo, Phys. Lett. **17**, 352 (1969)
- [3] S.J. Brodsky and A.H. Mueller, Phys. Lett. **B 206**, 685 (1988).
- [4] N.C.R. Makins *et al.*, Phys. Rev. Lett. **72**, 1986 (1994); T.G. O'Neill *et al.*, Phys. Lett. **351**, 87 (1995).
- [5] K. Garrow *et al.*, Phys. Rev. C **66**, 044613 (2002)
- [6] A.S. Carroll *et al.*, Phys. Rev. Lett. **61**, 1698 (1988)
- [7] Y. Mardor *et al.*, Phys. Rev. Lett. **81**, 5085 (1998); A. Leksanov *et al.*, Phys. Rev. Lett. **87**, 212301 (2001)
- [8] D. Dutta, R. Ent, K. Garrow, *et al.*, Jefferson Lab Hall C Experiment E-01-107, approved with A- priority and expected to run in 2004

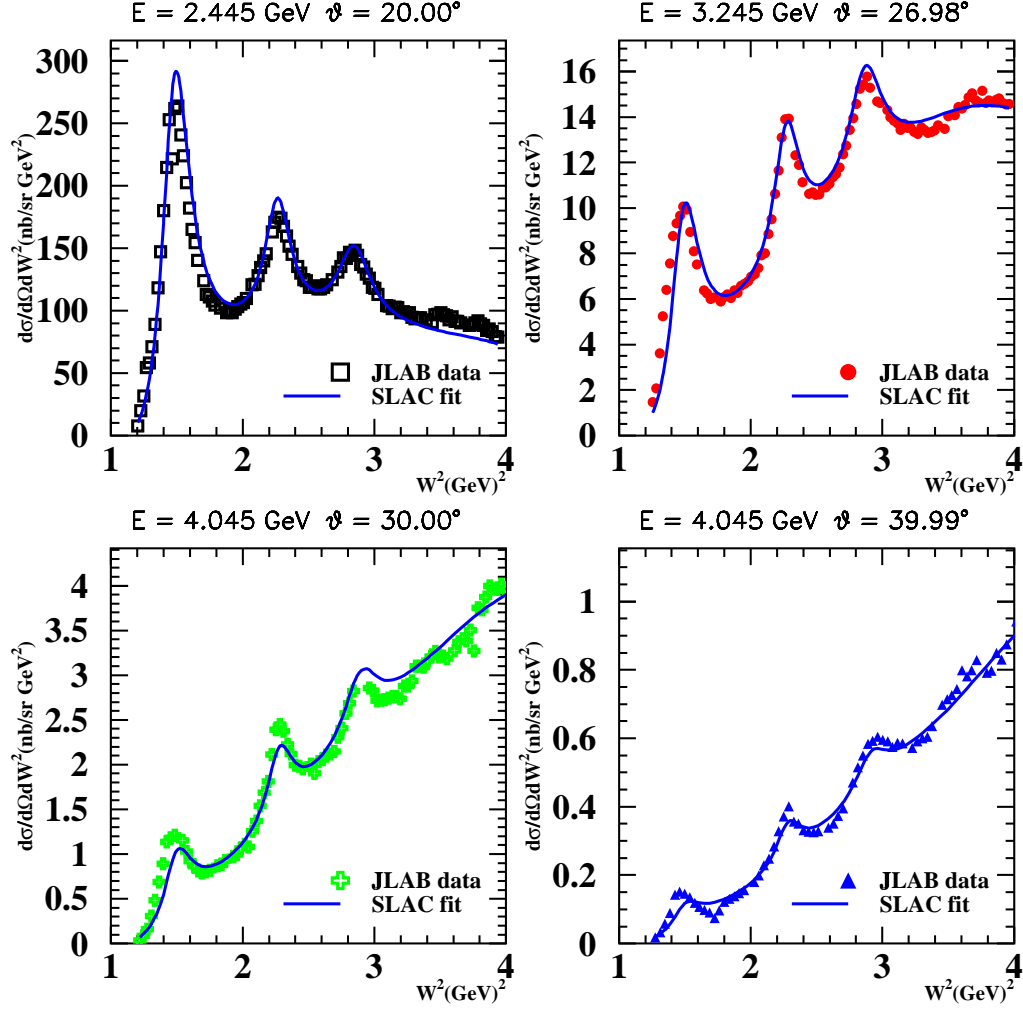


Figure 1: Inclusive electron scattering showing  $\Delta$  and higher resonances.  $Q^2$  at the  $\Delta$  peak is approximately 0.5, 1.5, 2.5 and 3.5 (GeV/c)<sup>2</sup> for the four spectra respectively

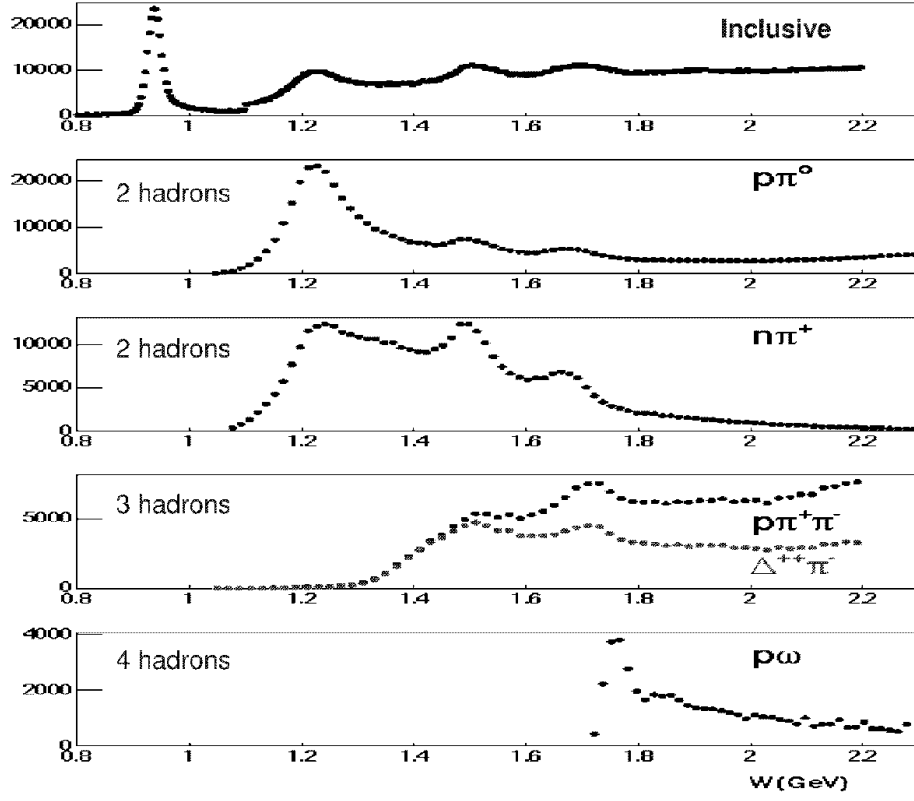


Figure 2: Invariant mass spectra from  $p(e, e'X)$  demonstrating the multi-hadron reconstruction capability in the JLab CLAS spectrometer.[?]

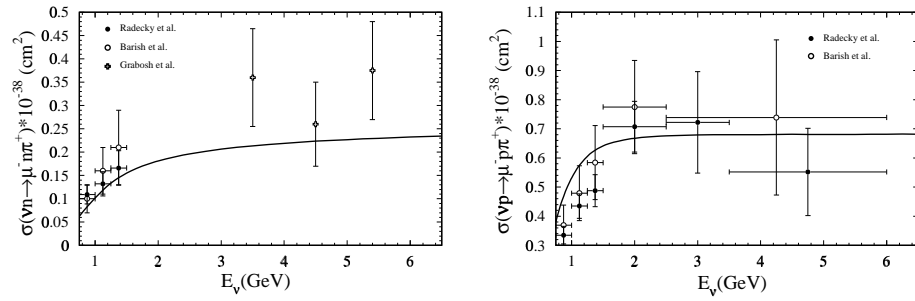


Figure 3: Total pion production cross sections.

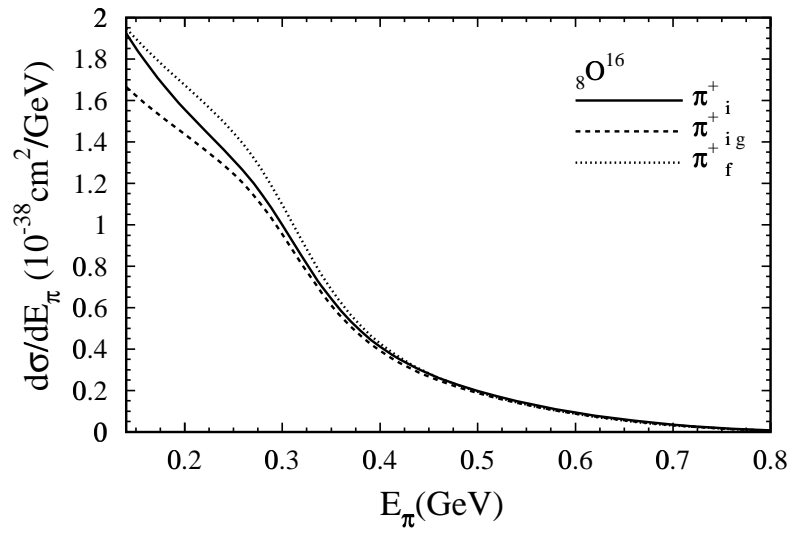


Figure 4: Predicted  $\pi^+$  energy distribution for  $\nu_\mu$  scattering on  $^{16}\text{O}$  of Paschos et. al.[?].

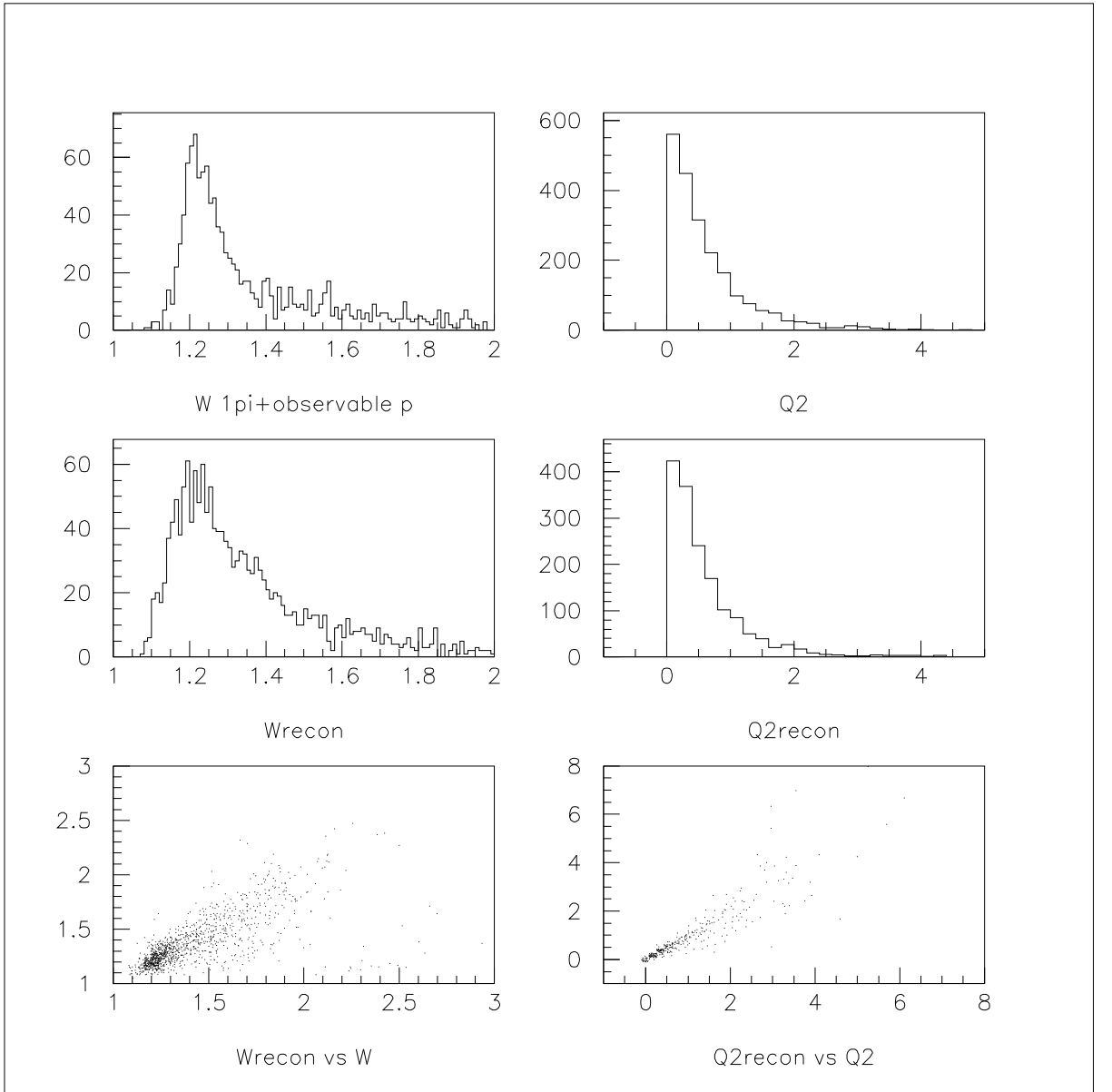


Figure 5:  $W$  and  $Q^2$  reconstruction for events with a single  $\pi^+$ . Top row are “true”  $W$  and  $Q^2$  distributions from the MINER $\nu$ A Monte Carlo. The second row are the reconstructed distributions assuming hadron energy resolutions from Figure 6. The invariant mass of the pion and highest energy proton give  $W$  which along with the muon energy and direction gives sufficient information to reconstruct  $Q^2$ . Bottom row shows the correlation between the “true” and reconstructed quantities.

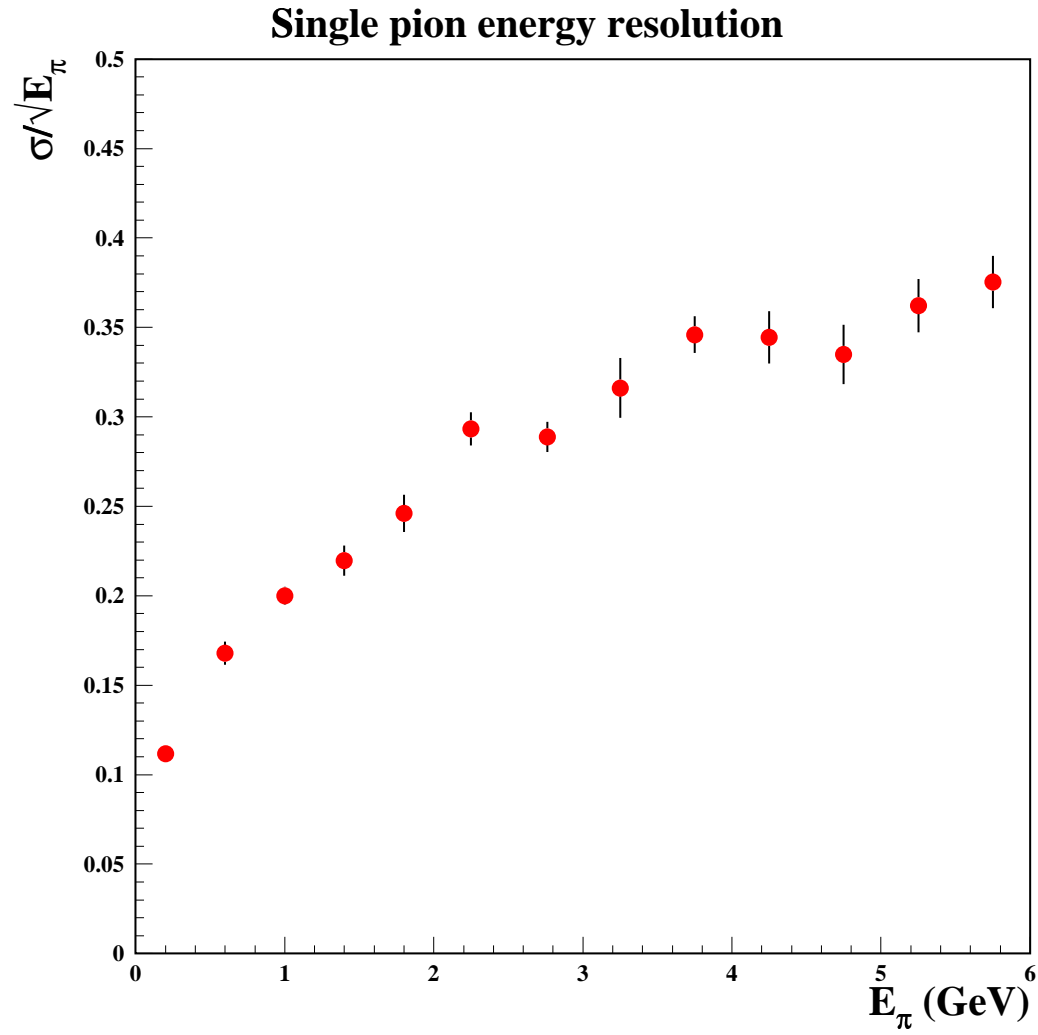


Figure 6: Single charged pion resolution derived from MINER $\nu$ A Monte Carlo.

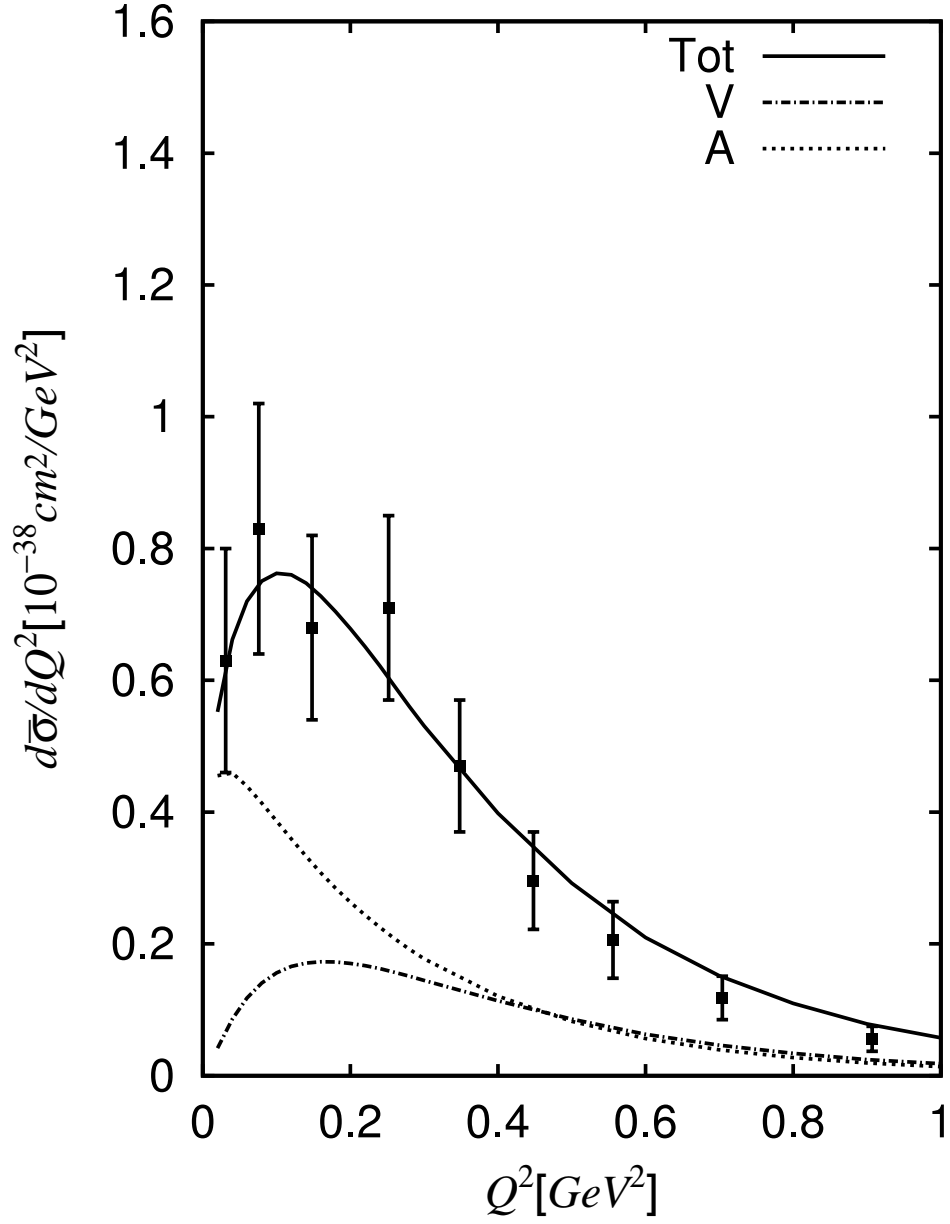


Figure 7: Differential cross section  $d\sigma/dQ^2$  ( $10^{-38}cm^2/GeV^2$ ) of  $p(\nu_\mu, \mu^- \pi^+)p$  averaged over neutrino energies. Calculations from Ref. [?], data from Ref. [?].